Available online at www.sciencedirect.com
SCIENCE DIRECT®
Journal of Solid State Chemistry 177 (2004) 2850–2854
JOURNAL OF SOLID STATE CHEMISTRY
http://elsevier.com/locate/jssc

Structural and electrical properties of $(1-x)(Na_{1/2}Bi_{1/2})TiO_3-xPb(Mg_{1/3}Nb_{2/3})O_3$ solid solution

Jung-Kun Lee,[a,*] Jae Yun Yi,[b] and Kug Sun Hong[b]

[a] *Los Alamos National Laboratory, Materials Science & Technology Division, ESA Energy and Process Engineering, MS J580 ESA-EPA, Los Alamos, NM 87545, USA*

[b] *School of Materials Science & Engineering, Seoul National University, Seoul 151-742, South Korea*

Received 6 January 2004; received in revised form 29 March 2004; accepted 26 April 2004

Abstract

Structural, dielectric and piezoelectric properties of $(1-x)(Na_{1/2}Bi_{1/2})TiO_3-xPb(Mg_{1/3}Nb_{2/3})O_3$ (NBT–*x*PMN) solid solution have been investigated. An addition of PMN into NBT transformed the structure of sintered samples from rhombohedral to pseudocubic phase where x is larger than 0.1. In calcined powders, however, the intermediate structure were observed between rhombohedral and cubic phases near $x=0.1$. The formation of solid solution between NBT and PMN modified the dielectric and piezoelectric properties of NBT to be suitable for high temperature dielectric and piezoelectric material. With increasing the content of PMN, the temperature-stability of $\varepsilon_r(T)$ increased and the high temperature dielectric loss decreased. In addition, the piezoelectric property of NBT–*x*PMN was enhanced, for the decrease of coercive field and conductivity promoted the domain reversal under the high electric field of the poling process.
© 2004 Elsevier Inc. All rights reserved.

Keywords: Sodium bismuth titanate; Phase transition; Piezoelectricity

1. Introduction

Sodium bismuth titanate, $(Na_{1/2}Bi_{1/2})TiO_3$ (NBT), is a typical *A*-site complex perovskite ferroelectric, which has received much interest due to its possible applications for piezoelectric, pyroelectric and high-temperature dielectric material. The most attractive features of NBT-based materials are (1) multiple phase transitions making it possible to control the temperature stability of the electrical property via the compositional modification, (2) high mechanical strength, (3) lack of air pollution from the lead volatilization, and (4) free control of toxic atmosphere during the sintering [1,2]. However, the wide applications of NBT have been limited for the high coercive field and the high conductivity of NBT. Coercive field of NBT is very close to its breakdown voltage, which prevents the complete domain reversal under high electric field of the poling process. High conductivity of NBT responsible for space charge polarization above 200°C, is also undesirable for the dielectric and piezoelectric application, even though the mechanism of high conduction is not clear yet. To make up for these shortcomings, the compositional modification of NBT using $PbTiO_3$, $SrTiO_3$, $BaTiO_3$, $PbZrO_3$ and rare-earth elements have been performed for decades [3–7].

$Pb(Mg_{1/3}Nb_{2/3})O_3$ (PMN) is a typical relaxor ferroelectrics which have a diffuse phase transition. Above the room temperature, PMN has a very slim polarization and strain vs. electric field ($P-E$) curve with a small coercive field. In addition, the dielectric loss of PMN decreases rapidly above the room temperature [8,9]. Therefore, it is expected that addition of PMN compensate the shortcomings of NBT; high coercive field and high conductivity. In view of this, the present study is focused on studying the crystal structure, phase transition behavior, and electrical properties of $(1-x)(Na_{1/2}Bi_{1/2})TiO_3-xPb(Mg_{1/3}Nb_{2/3})O_3$ (NBT–*x*PMN) solid solutions.

2. Experimental procedures

$(1-x)(Na_{1/2}Bi_{1/2})TiO_3-xPb(Mg_{1/3}Nb_{2/3})O_3$ (NBT–*x*PMN) solid solution samples ($0\leqslant x\leqslant 1$) were prepared

*Corresponding author. Fax: +1-505-667-8779.
E-mail address: jklee@lanl.gov (J.-K. Lee).

0022-4596/$ - see front matter © 2004 Elsevier Inc. All rights reserved.
doi:10.1016/j.jssc.2004.04.046

Table 1
Composition of $(1-x)(Na_{1/2}Bi_{1/2})TiO_3$–$xPb(Mg_{1/3}Nb_{2/3})O_3$ ceramics which were sintered at 1150°C

Nominal composition	Element (mol %)					
	Na (%)	Bi (%)	Ti (%)	Pb (%)	Mg (%)	Nb (%)
NBT	25	25	50	0	0	0
NBT–0.3PMN	17	15	35	16	7	10
NBT–0.7PMN	7	5	14	32	15	27
PMN	0	0	0	50	17	33

using mixed oxide method. Reagent-grade Na_2CO_3, Bi_2O_3, TiO_2, PbO, MgO and Nb_2O_5 were used as starting materials. Starting materials were weighed and mixed by ball-milling for 24 h with stabilized zirconia media and ethanol. After drying, the mixed powder was calcined at 800°C for 2 h. The calcined powder was ground by ball-milling for 24 h. The milled powder was then uniaxially pressed into pellets at a pressure of 1000 kg/cm^2 using polyvinyl alcohol (PVA). The pellets whose diameter and thickness were 20 and 1 mm, were sintered at 1150°C for 2 h in air.

Crystal structure of solid solutions was investigated using X-ray powder diffraction in the 2θ range of 10–60° using Cu$K\alpha$ radiation (Model M18XHF, Macscience Instruments, Japan). A scanning step size and a counting time were of 0.04° and 1 s/step, respectively. The composition of NBT–xPMN ceramics was measured using quantitative analysis by electron probe micro-analysis (EPMA, Model JXA-8900R, JEOL, Japan) and the results were summarized in Table 1. The composition of NBT–xPMN ceramics in grains was similar to the nominal composition, suggesting that the reaction produced the complete solid solutions between NBT and PMN.

Fire-on silver paste was used as the electrode for the electrical measurement. The dielectric constant versus temperature $[\varepsilon_r(T)]$ curve was measured at temperatures ranging from room temperature to 450°C with a heating rate of 100°C/h using an impedance analyzer (Hewlett-Packard, Model 4192A, USA). Specimens for piezoelectric measurements were poled in a silicone oil bath with a DC field of 60 kV/cm for 15 min at 50°C and was cooled down to room temperature under a DC field. Piezoelectric properties were measured using the resonance–antiresonance method (IEEE standard No. 176-1978).

3. Result and discussion

3.1. Crystal structure

Fig. 1 shows the crystal structure of NBT–xPMN ceramics sintered at 1150°C. In pure NBT, the

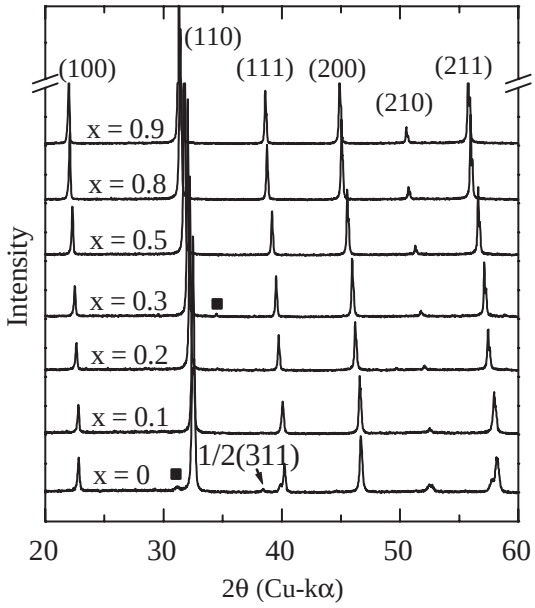

Fig. 1. XRD patterns of $(1-x)(Na_{1/2}Bi_{1/2})TiO_3-xPb(Mg_{1/3}Nb_{2/3})TiO_3$ ceramics which were sintered at 1150°C ($x = 0$, 0.1, 0.2, 0.3, 0.5, 0.8, 0.9); (■) denotes the second phase.

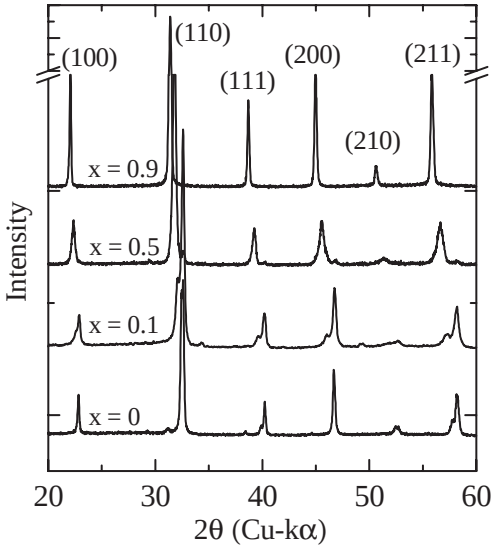

Fig. 2. XRD patterns of $(1-x)(Na_{1/2}Bi_{1/2})TiO_3-xPb(Mg_{1/3}Nb_{2/3})TiO_3$ powders which were calcined at 850°C ($x = 0$, 0.1, 0.5, 0.9).

rhombohedral distortion and the superlattice reflection from the anti-phase tilting of the oxygen octahedral of NBT were observed. Since the macroscopic structure of PMN is cubic at room temperature, the rhombohedral lattice distortion of NBT decreased with increasing the PMN content and the structure of the solid solution transformed into pseudo-cubic phase where x is larger than 0.1. XRD patterns of calcined powder in Fig. 2, however, show that the crystal structure of calcined

powders is different from that of sintered samples. In a composition of $x = 0.1$, both (111) and (200) reflections showed the apparent peak split. Assuming that the samples are complete solid solution, the split of reflections in both (111) and (200) indicates that the addition of PMN into NBT caused either (1) the coexistence of rhombohedral and tetragonal phases or (2) the phase transition into lower crystal symmetry phase such as the monoclinic structure in the calcined powder when a small amount of PMN was added. The peak splits in calcined powders decreased with increasing the content of PMN and the deviation from cubic structure was not observed for the calcined powder with $x > 0.3$. Despite the lack of the macroscopic distortion, full-width at half-maximum (FWHM) of a composition of $x = 0.5$ was still broader than that of PMN. This indicates that the calcined power of NBT–0.5PMN still has the non-uniform lattice distortion and internal stress though the macroscopic distortion was not detected under the resolution of XRD [10,11]. To clarify the presence of addition lattice distortion in calcined powders for lower PMN content, more XRD measurements were performed for NBT–0.1PMN samples that were annealed at 700°C, 850°C, and 1150°C. As shown in Fig. 3, the peak split as an evidence of transient phase transition was clearly observed in peaks such as (111) and (300) reflections and the degree of the transient lattice distortion of NBT–0.1PMN became pronounced with increasing the calcinations temperature in the range 700°C–850°C. The crystal structure of NBT–xPMN is interesting for there is transient morphotropic phase transition to either the coexistence of tetragonal and rhombohedral phases or monoclinic structure only near 800°C, which is not observed in sintered samples. The origin of the transient tetragonal lattice distortion near $x = 0.1$ below 850°C is not yet clear and further investigation is under progress using single crystals.

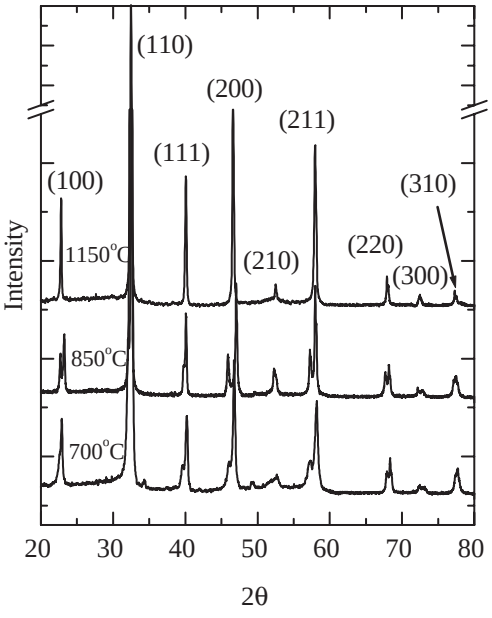

Fig. 3. XRD patterns of $0.9(Na_{1/2}Bi_{1/2})TiO_3-0.1Pb(Mg_{1/3}Nb_{2/3})TiO_3$ powders which were heat-treated at 700°C, 850°C, and 1150°C.

3.2. Phase transition

$\varepsilon_r(T)$ of NBT–xPMN solid solutions at 100 kHz is shown in Fig. 4. It demonstrates that the phase transition was broadened with increasing the content of PMN. The temperature of maximum permittivity decreased about 25°C per the addition of 10 mol% PMN. Decrease in the maximum permittivity temperature, in turn, increased the room temperature dielectric constant of NBT–xPMN solid solution. Fig. 5 shows dielectric loss of NBT–xPMN solid solutions at 100 kHz. Large dielectric loss at high temperature was suppressed by increasing PMN content. Since the high dielectric loss of NBT near 300°C is attributed to the extrinsic factor such as mobile ions, this result shows that the addition of PMN provides the effective barrier for the movement of mobile ions of NBT [12,13]. One of the weakness of NBT for the application of high temperature dielectric materials is large dielectric loss and conduction at high temperature [3,4]. Hence, the low dielectric loss shown in Fig. 4, indicates that the addition of PMN compensates one of the weaknesses of NBT.

Fig. 6 shows the frequency dependence of the permittivity as a function of temperature for NBT and NBT–0.2PMN. Compared to $\varepsilon_r(T)$ of NBT, that of NBT–0.2PMN clearly shows two phase successive transitions at 75°C and 240°C. Between two phase transition temperatures (75°C and 240°C), the variation of the permittivity as a function of temperature becomes

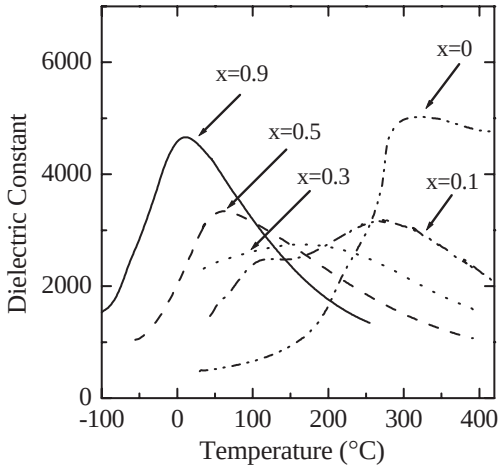

Fig. 4. Temperature dependence of the permittivity for $(1-x)(Na_{1/2}Bi_{1/2})TiO_3-xPb(Mg_{1/3}Nb_{2/3})O_3$ ceramics which were measured at 100 kHz ($x = 0$, 0.1, 0.3, 0.5, and 0.9).

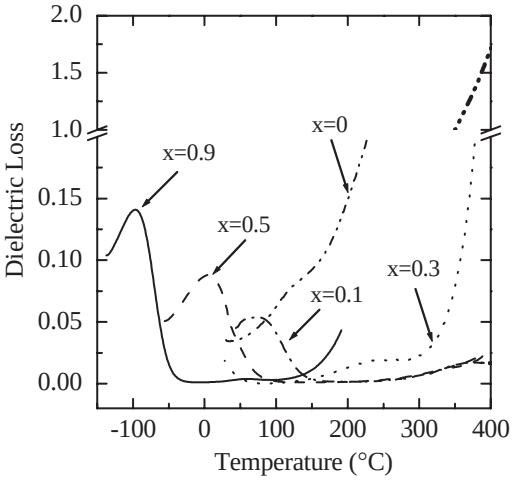

Fig. 5. The temperature dependence of the dielectric loss in $(1-x)(Na_{1/2}Bi_{1/2})TiO_3-xPb(Mg_{1/3}Nb_{2/3})O_3$ ceramics which were measured at 100 kHz ($x = 0$, 0.1, 0.5, and 0.9).

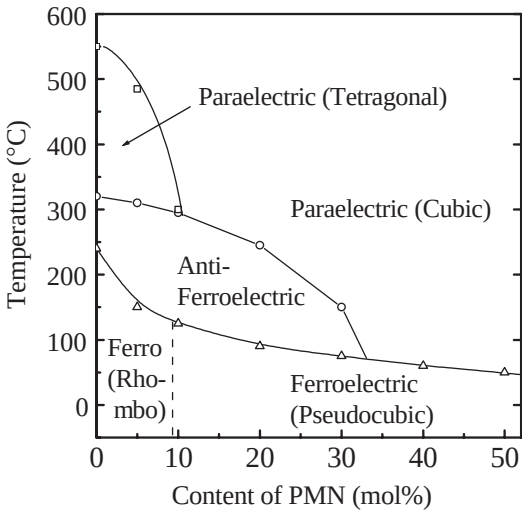

Fig 7. Phase diagram of $(1-x)(Na_{1/2}Bi_{1/2})TiO_3-xPb(Mg_{1/3}Nb_{2/3})O_3$ ceramics which were sintered at 1150°C.

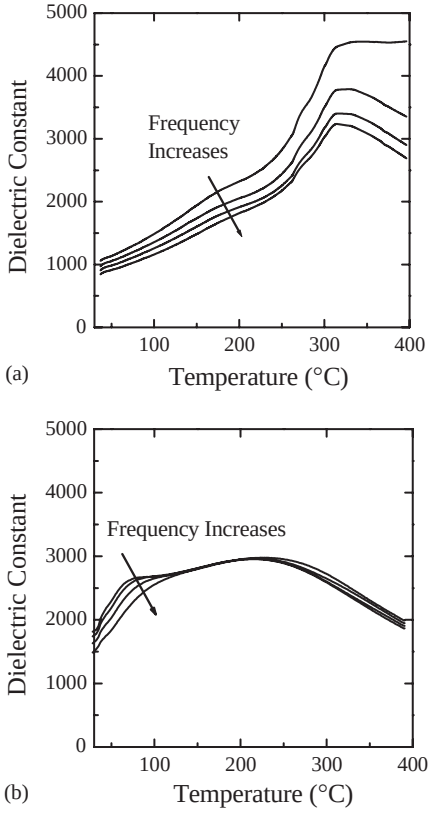

Fig. 6. Temperature dependence of the dielectric constant measured at 1, 10, 100, 1000 kHz; (a) $(Na_{1/2}Bi_{1/2})TiO_3$ and (b) $0.8(Na_{1/2}Bi_{1/2})TiO_3-0.2Pb(Mg_{1/3}Nb_{2/3})O_3$ ceramics.

flat, which is suitable for the high temperature dielectrics. Another interesting feature of $\varepsilon_r(T)$ for NBT–0.2PMN is that the $\varepsilon_r(T)$ shows the strong frequency dispersion near 75°C, while the phase transition near 240°C does not depend on the measuring frequency. The previous research on the ferroelectricity and cation ordering of NBT suggested the possibility that NBT has two successive phase transitions with a sequence of ferroelectric–incommensurate antiferroelectric–paraelectric phases with increasing temperature, analogous to other highly ordered perovskites such as $Pb(Co_{1/2}W_{1/2})O_3$ and $Pb(Yb_{1/2}Ta_{1/2})O_3$ [14–16]. The results of this study show that the addition of PMN could manifest the inherent and complicate phase transition of NBT.

Based on the experimental observation and discussion of this study, phase diagram was presented in Fig. 7 for $(1-x)(Na_{1/2}Bi_{1/2})TiO_3-xPb(Mg_{1/3}Nb_{2/3})O_3$ ceramics which were sintered at 1150°C. The detailed study on the structure of intermediate antiferroelectric phase is under progress using the transmission electron microscopy (TEM).

3.3. Piezoelectric property

The piezoelectric properties of NBT–xPMN solid solutions are summarized in Table 2. It shows that the piezoelectric properties of NBT–xPMN varied nonlinearly as a function of PMN content. The piezoelectric coefficient (d_{33}) of NBT–xPMN increased from 55 pC/N (NBT) to 89 pC/N (NBT–0.2PMN). The enhancement of d_{33} resulted in the increase of the piezoelectric coupling coefficient. The thickness and planar coupling coefficients of NBT–xPMN changed from 12%, 41% (NBT) to 17%, 50% (NBT–0.2PMN). When x was larger than 0.2, the piezoelectric property decreased with increasing the content of PMN. Since the relative density of samples sintered at 1150°C was higher than 95%, the effect of the microstructure on the change in the piezoelectric coefficients is not significant and this

Table 2
Piezoelectric properties of $(1-x)(Na_{1/2}Bi_{1/2})TiO_3$–$xPb(Mg_{1/3}Nb_{2/3})O_3$ ceramics which were sintered at 1150°C ($x = 0.1, 0.2, 0.3, 0.4$)

	k_p (%)	k_t (%)	d_{33} (pC/N)	ε_{33}
NBT	12	41	55	260
NBT–0.1PMN	14	45	71	870
NBT–0.2PMN	17	49	89	1250
NBT–0.3PMN	13	43	65	2035
NBT–0.4PMN	12	39	61	2640

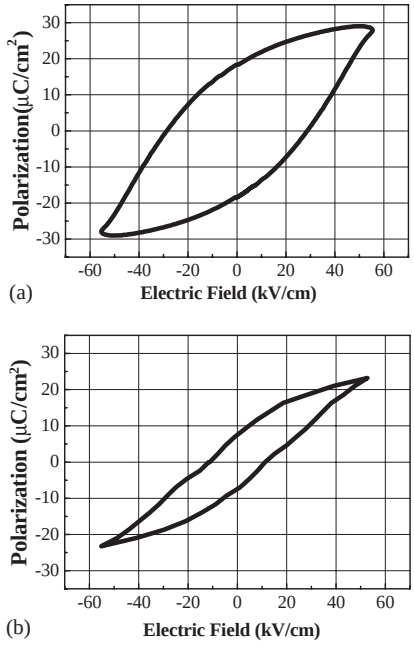

Fig. 8. Hysteresis loops for $(1-x)(Na_{1/2}Bi_{1/2})TiO_3-xPb(Mg_{1/3}Nb_{2/3})O_3$ ceramics at room temperature: (a) $x = 0$, and (b) $x = 0.3$.

enhanced piezoelectricity by the addition of PMN is attributed to effective domain reversal under the high electric field during the poling process [5,17]. Fig. 8 shows the hysteresis loops for NBT–xPMN solid solutions, which demonstrates that the coercive field decreased with increasing the PMN content. Since the addition of PMN decreases high coercive field of NBT and prevents the movement of mobile ions of NBT, NBT–xPMN solid solution becomes piezoelectrically soft and the efficiency for the response of domains to the external field increases for PMN modified NBT. Hence, the addition of PMN enhances the piezoelectric property of NBT–xPMN solid solutions. When the content of PMN was above 30 mol%, the piezocoefficients of NBT–xPMN solid solutions decreased. This adverse effect for higher amount of PMN may result from the decrease of effective dipole moments for the small remnant polarization of PMN.

4. Conclusion

(1) An addition of PMN into NBT transformed the structure of sintered samples from rhombohedral to pseudocubic phase. However, the phase transition behavior of calcined powder was different from that of sintered samples. When the content of added PMN was less than 20 mol%, the tetragonal phase was found transiently in powder calcined from 700°C to 850°C.

(2) As the content of PMN increased, the temperature-stability of $\varepsilon_r(T)$ of NBT–xPMN increased and the dielectric loss of NBT–xPMN at high temperature decreased. In NBT–0.2PMN, $\varepsilon_r(T)$ showed the constant variation of the permittivity between two successive phase transitions. It indicates the possibility of NBT–xPMN for the high temperature dielectrics.

(3) The piezoelectric property of NBT was enhanced by the addition of PMN. The thickness coupling coefficient, planar coupling coefficient and piezoelectric coefficient were maximized ($k_t = 49\%$, $k_p = 17\%$, $d_{33} = 89\,p$C/N) at NBT–0.2PMN. It is postulated that the addition of PMN promotes the piezoelectric response by decreasing the coercive field and the dielectric loss of NBT.

References

[1] G.A. Smolenski, V.A. Isupov, R.I. Agranovskaya, N.N. Kainik, Sov. Phys. Solid State 2 (1961) 2651–2654.
[2] H. Nagata, T. Takenaka, Jpn. J. Appl. Phys. 36 (1997) 6055–6057.
[3] K. Sakata, T. Takenaka, Y. Naitou, Ferroelectrics 131 (1992) 219–226.
[4] K. Sakata, Y. Masuda, Ferroelectrics 7 (1974) 347–349.
[5] A. Herabut, A. Safari, J. Am. Ceram. Soc. 80 (1997) 2954–2958.
[6] J.K. Lee, K.S. Hong, S.-E. Park, C.K. Kim, J. Appl. Phys. 91 (2002) 4538–4542.
[7] J.K. Lee, K.S. Hong, Jpn. J. Appl. Phys. 40 (2001) 6003–6007.
[8] S.M. Pilgrim, M. Massuda, J.D. Prodey, A.P. Ritter, J. Am. Ceram. Soc. 75 (1992) 1964–1969.
[9] J.H. Park, B.K. Kim, S.J. Park, J. Am. Ceram. Soc. 79 (1996) 430–434.
[10] S.E. Park, K.S. Hong, J. Mater. Res. 12 (1997) 2152–2157.
[11] C.N.W. Darlington, J. Phys. C 21 (1988) 3851–3861.
[12] J.Y. Yi, J.K. Lee, K.S. Hong, J. Am. Ceram. Soc. 85 (2002) 3004–3010.
[13] S.-E. Park, S-J. Chung, I.-T. Kim, J. Am. Ceram. Soc. 79 (1996) 1290–1296.
[14] C.-S. Tu, I.G. Siny, V.H. Schmidt, Phys. Rev. B 49 (1994) 11550–11558.
[15] N. Yasuda, J. Konda, Appl. Phys. Lett. 62 (1993) 535–537.
[16] C.A. Randall, S.A. Markgraf, A.S. Bhalla, K. Baba-Kishi, Phys. Rev. B 40 (1989) 413–416.
[17] M.S. Hagiyev, I.H. Ismailzade, A.K. Abiyev, Ferroelectrics 56 (1984) 215–217.